Citation: **Hirt, C**, S.J. Claessens, T. Fecher, M. Kuhn, R. Pail, M. Rexer (2013), New ultra-high resolution picture of Earth's gravity field, *Geophysical Research Letters*, Vol 40, doi: 10.1002/grl.50838.

New ultra-high resolution picture of Earth's gravity field

Christian Hirt[1*], Sten Claessens[1], Thomas Fecher[2], Michael Kuhn[1], Roland Pail[2], Moritz Rexer[1, 2]
[1] Western Australian Centre for Geodesy, Curtin University, Perth, Australia
[2] Institute for Astronomical and Physical Geodesy, Technical University Munich, Germany
* E-mail: c.hirt@curtin.edu.au

Abstract

We provide an unprecedented ultra-high resolution picture of Earth's gravity over all continents and numerous islands within ± 60 degree latitude. This is achieved through augmentation of new satellite and terrestrial gravity with topography data, and use of massive parallel computation techniques, delivering local detail at ~200 m spatial resolution. As such, our work is the first-of-its-kind to model gravity at unprecedented fine scales yet with near-global coverage. The new picture of Earth's gravity encompasses a suite of gridded estimates of gravity accelerations, radial and horizontal field components and quasigeoid heights at over 3 billion points covering 80% of Earth's land masses. We identify new candidate locations of extreme gravity signals, suggesting that the CODATA standard for peak-to-peak variations in free-fall gravity is too low by about 40%. The new models are beneficial for a wide range of scientific and engineering applications and freely available to the public.

Keywords

Earth's gravity field, gravity, quasigeoid, vertical deflections, ultra-high resolution

1 Introduction

Precise knowledge of the Earth's gravity field structure with high resolution is essential for a range of disciplines, as diverse as exploration and potential field geophysics [*Jakoby and Smilde*, 2009], climate and sea level change research [*Rummel*, 2012], surveying and engineering [*Featherstone*, 2008] and inertial navigation [*Grejner-Brzezinska and Wang*, 1998]. While there is a strong scientific interest to model Earth's gravity field with ever-increasing detail, the resolution of today's gravity models remains limited to spatial scales of mostly 2-10 km globally [*Pavlis et al.*, 2012; *Balmino et al.*, 2012], which is insufficient for local gravity field applications such as modelling of water flow for hydro-engineering, inertial navigation or in-situ reduction of geophysical gravity field surveys. Up until now, gravity models with sub-km resolution are unavailable for large parts of our planet.

Here we provide an unprecedented ultra-high resolution view of five components of Earth's gravity field over all continents, coastal zones and numerous islands within ±60 degree latitude. This is achieved through augmentation of new satellite and terrestrial gravity with topography data [e.g., *Hirt et al.* 2010] and use of massive parallel computation techniques, delivering local detail at 7.2 arc-seconds (~200 m in North-South direction) spatial resolution (Section 2). As such, our work is the first-of-its-kind to model gravity at ultra-fine scales yet with near-global coverage. The new picture of Earth's gravity encompasses a suite of gridded estimates of gravity accelerations, radial and horizontal field components and quasigeoid heights at over 3 billion points covering 80% of Earth's land masses and 99.7% of populated areas (Section 3, 4). This considerably extends our current knowledge of the gravity field. The gridded estimates are beneficial for a range of scientific and engineering applications (Section 5) and freely available to the public. Electronic supplementary materials are available providing full detail on the methods applied in this study.

2 Data and Methods

Our ultra-high resolution picture of Earth's gravity field is a combined solution based on the three key constituents GOCE/GRACE satellite gravity (providing the spatial scales of ~10000 down to ~100 km), EGM2008 (~100 to ~10 km) and topographic gravity, i.e., the gravitational effect implied by a high-pass filtered terrain model (scales of ~10 km to ~250 m),

Regarding the satellite component, we use the latest satellite-measured gravity data (release GOCE-TIM4) from the European Space Agency's GOCE satellite [*Drinkwater et al*., 2003; *Pail et al.*, 2011], parameterized as coefficients of a spherical harmonic series expansion, that currently provides the highest-resolution picture of Earth's gravity ever obtained from a space gravity sensor. Resolving gravity field features at spatial scales as short as 80-100 km, GOCE confers new gravity field knowledge, most notably over poorly surveyed regions of Africa, South America and Asia [*Pail et al.*, 2011].

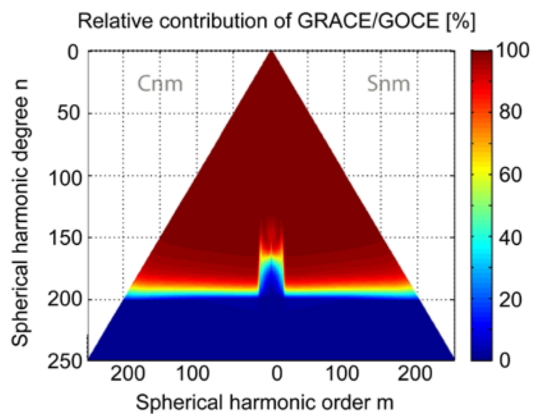

Figure 1. Relative contribution of GOCE/GRACE data per spherical harmonic coefficient in the combination with EGM2008 data (in percent) for the degrees 0 to 250

Compared to pure GOCE models, complementary GRACE satellite gravity [*Mayer Guerr et al.*, 2010] are superior in the spectral range up to degrees 70-80 [*Pail et al.*, 2010]. Therefore, first a combined satellite-only combined solution based on full normal equations of GRACE (up to degree 180) and GOCE (up to degree 250) is computed [see, e.g., *Pail et al.*, 2010]. The GRACE/GOCE combination is then merged with EGM2008 [*Pavlis et al.*, 2012] using the EGM2008 coefficients as pseudo-observations. Since for EGM2008 only the error variances are available, the corresponding normal equations have diagonal structure. In our combination, GRACE/GOCE data have dominant influence in the spectral band of harmonic degrees 0 to 180 with EGM2008 information taking over in the spectral range 200 to 2190, leaving the main spectral range of transition from GRACE/GOCE to EGM2008 in spectral band of degrees 181 to

200. The relative contributions of EGM2008 and GRACE/GOCE satellite gravity are shown in Fig. 1.

The spherical-harmonic coefficients of the combined GRACE/GOCE/EGM2008 (GGE) gravity model were used in the spectral band of degrees 2 to 2190 to synthesize a range of frequently used gravity field functionals at the Earth's surface. For accurate spherical harmonic synthesis at the Earth's surface, as represented through the SRTM topography, the gradient approach to fifth-order [*Hirt* 2012] was applied. This numerically efficient evaluation technique takes into account the effect of gravity attenuation with height. Applying the gradient approach as described in *Hirt* [2012] yielded numerical estimates for radial derivatives (gravity disturbances) and horizontal derivatives (deflections of the vertical) of the disturbing potential and quasigeoid heights from the GGE data set at 7.2 arc-sec resolution (about 3 billion surface points) within the SRTM data coverage.

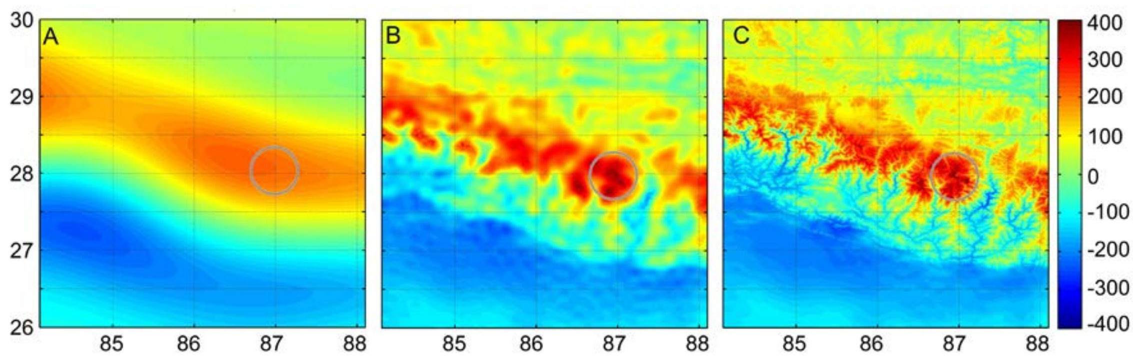

Figure 2. Gravity field at different levels of resolution over Mount Everest area. A: satellite-only (free-air) gravity from GOCE and GRACE satellites, B: GGE gravity (satellite gravity combined with EGM2008 gravity), C: GGMplus as composite of satellite gravity, EGM2008 and topographic gravity. Shown is the radial component of the gravity field over a ~400 x 400 km area covering parts of the Southern Himalayas including the Mount Everest summit area (marked), units in 10^{-5} m s^{-2}. The spatial resolution of the gravity modelling increases from ~100 km (A), ~10 km (B) to ultra-fine ~200 m spatial scales (C).

For the Mount Everest region, Fig. 2 exemplifies the associated resolution of GOCE/GRACE satellite gravity (A) and their combination with EGM2008 gravity (B). The spatial resolution of the GGE gravity field functionals is limited to about ~10 km (or harmonic degree of 2190) which leaves the problem of modelling the field structures at short scales, down to few 100 m resolution at any of the surface points.

Because ground gravity measurements at a spatial density commensurate with our model resolution do not exist over most parts of Earth [e.g., *Sansò and Sideris,* 2013] – and will not become available in the foreseeable future – alternative solutions are required to estimate the gravity field signals at scales shorter than 10 km. High-resolution topography data is widely considered the key to ultra-high resolution gravity modelling and used successfully as effective means to estimate short-scale gravity effects [*Sansò and Sideris,* 2013; *Tziavos and Sideris*, 2013, *Pavlis et al.,* 2012; *Forsberg and Tscherning*, 1981]. This is because the short-scale gravity field is dominated by the constituents generated by the visible topographic masses

[*Forsberg and Tscherning*, 1981]. However, forward estimation of the short-scale gravity field constituents from elevation models near-globally at ultra-high (few 100 metres) resolution is computationally demanding. Yet we have accomplished this challenge for the first time through advanced computational resources.

Massive parallelization and the use of Western Australia's iVEC/Epic supercomputing facility allowed us to convert topography from the Shuttle Radar Topography Mission (SRTM), cf. *Jarvis et al.* [2008] – along with bathymetric information along coastlines [*Becker et al.*, 2009] – to topographic gravity at 7.2 arc-sec resolution everywhere on Earth between ± 60° latitude with SRTM data available. Based on non-parallelized standard computation techniques, the calculation of topographic gravity effects would have taken an estimated 20 years, which is why previous efforts were restricted to regional areas [*Kuhn et al.*, 2009; *Hirt*, 2012].

The conversion of topography to topographic gravity is based on the residual terrain modelling technique [*Forsberg*, 1984], with the topography high-pass filtered through subtraction of a spherical harmonic reference surface (of degree and order 2160) prior to the forward-modelling. We treated the ocean water masses and those of the major inland water bodies (Great Lakes, Baikal, Caspian Sea) using a combination of residual terrain modelling with the concept of rock-equivalent topography [*Hirt*, 2013], whereby the water masses were 'compressed' to layers equivalent to topographic rock. These procedures yield short-scale topographic gravity that is suitable for augmentation of degree-2190 spherical harmonic gravity models beyond their associated 10 km resolution, cf. *Hirt* [2010; 2013]. The topographic gravity is based on a mass-density assumption of 2670 kg m^{-3} and provides the spatial scales of ~10 km to ~250 m, which is complementary to the GGE gravity (spatial scales from ~10000 km to ~10 km).

3 Results

Addition of both components (GGE and topographic gravity) result in the ultra-high resolution model GGMplus (Global Gravity Model, with plus indicating the leap in resolution over previous 10 km resolution global gravity models). The modelled gravity field components and their descriptive statistics are reported in Table 1.

Table 1. Descriptive statistics of the GGMplus model components calculated at 3,062,677,383 land and near-costal points within ± 60° geographic latitude. RMS is the root-mean-square of the component.

Gravity model component		**Min**	**Max**	**RMS**	**Unit**
Gravity	Free-fall acceleration	976392	981974	980133	10^{-5} m s^{-2}
	Radial component	-456	714	48.0	10^{-5} m s^{-2}
Horizontal components	North-South	-108	94	6.9	arc-sec
	East-West	-83	79	6.8	arc-sec
	Total (magnitude)	0	109	9.4	arc-sec
Quasigeoid		-99.26	86.60	29.91	m

This world-first ultra-high resolution modelling over most of Earth's land areas delivered us the expected gravity signatures of small-scale topographic features – such as mountain peaks and valleys – which are otherwise masked in 10 km resolution models. This adds much local detail to the gravity maps (compare Figs. 2B and 2C) and yields a spectrally more complete and accurate description of the gravity field [e.g., *Hirt*, 2012].

Table 2. Candidate locations for extreme values of Earth's gravity field

Gravity component	**Minimum/ Maximum**	**Latitude/ Longitude**	**Geographic feature/ location**
Gravity acceleration	9.76392 m s^{-2}	-9.12°/ -77.60°	Huascarán, Peru
	9.83366 m s^{-2}	86.71°/61.29°	*Arctic Sea
Radial component	-456×10^{-5} m s^{-2}	29.71°/95.36°	Gandengxiang, China
	714×10^{-5} m s^{-2}	10.83°/-73.69°	Pico Cristóbal Colón, Columbia
Horizontal component+	109 arc-sec	28.45°/84.13°	~10 km South of Annapurna II, Nepal
Quasigeoid	-106.59 m	4.71°/78.79°	*Laccadive Sea, South of Sri Lanka
	86.60 m	-8.40°/147.35°	Puncak Trikora, Papua, Indonesia

* offshore area, value estimated without topographic gravity using GGE-only (10 km resolution, also see electronic supplement)

+ total component computed as magnitude from the North-South and East-West components

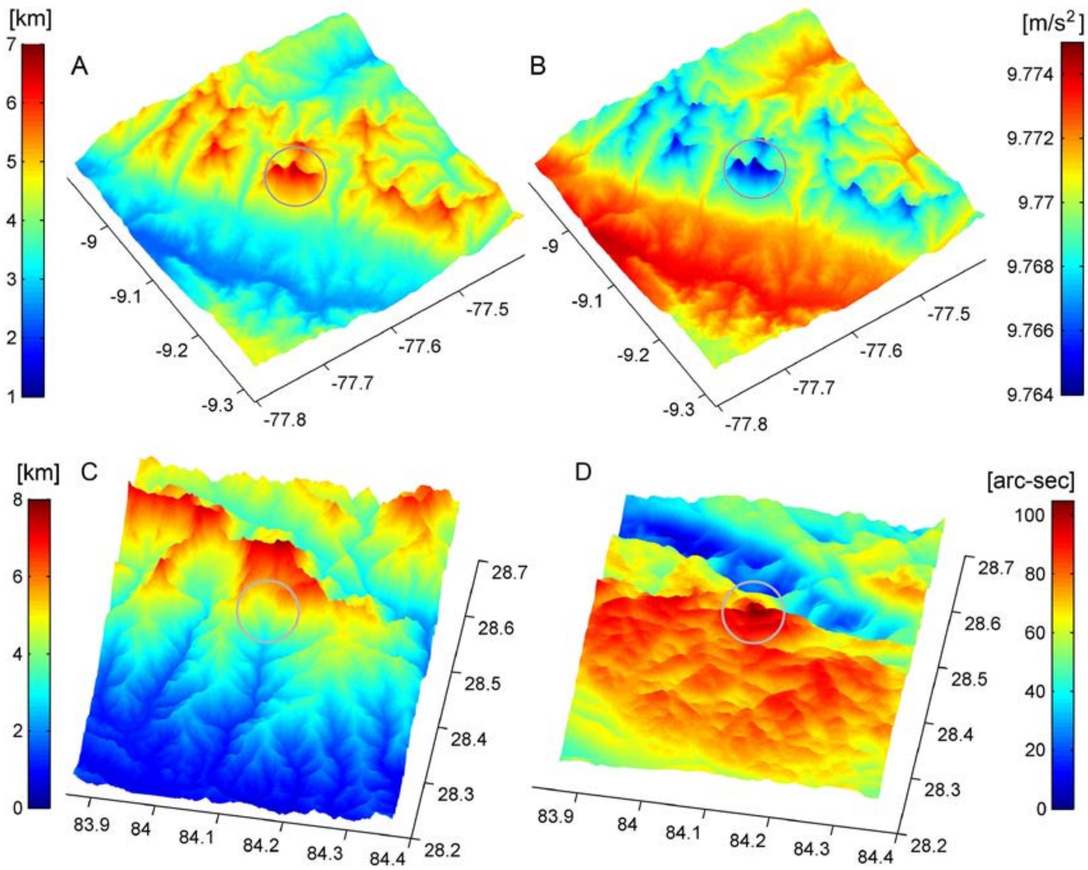

Figure 3. Candidate locations of some extreme signals in Earth's gravity in the Andes (A,B) and Himalaya regions (C,D). Top: Topography (A) and free-fall gravity accelerations (B) over the Huascarán region (Peru), where GGMplus gravity accelerations are as small as ~9.764 m s^{-2} (B). Bottom: Topography (C) and GGMplus total horizontal field component (D) over the Annapurna II region (Nepal). The gravitational attraction of the Annapurna II masses is expected to cause an extreme slope of the quasi/geoid with respect to the Earth ellipsoid of up to ~109 arc-seconds (D).

Our gridded estimates portray the subtle variations of gravity (Fig. 3) which are known to depend on factors such as location, height and presence of mass-density anomalies. GGMplus reveals a candidate location for the minimum gravity acceleration on Earth: the Nevado Huascarán summit (Peru) with an estimated acceleration of 9.76392 m s^{-2} (Fig 3A, 3B, and Table 2). A candidate location for Earth's maximum gravity acceleration was identified - outside the SRTM area, based on GGE-only – in the Arctic sea with an estimated 9.83366 m s^{-2}. This suggests a variation range (peak-to-peak variation) for gravity accelerations on Earth of about ~0.07 m s^{-2}, or 0.7 %, which is about 40 % larger than the variation range of 0.5 % implied by standard models based on a rotating mass-ellipsoid (gravity accelerations are 9.7803 m s^{-2} (equator) 9.8322 m s^{-2} (poles) on the mass-ellipsoid, cf. *Moritz* [2000]). So far such a simplified model is also used by the Committee on Data for Science and Technology (CODATA) to estimate the variation range in free-fall acceleration on Earth [*Mohr and Taylor*, 2005]. However, due to the inhomogeneous structure of Earth, presence of topographic masses, and decay of gravity with height the actual variations in free-fall accelerations are ~40% larger at the Earth's surface (Table 2).

GGMplus free-air gravity – the radial component of Earth's gravity field – varies within a range of ~0.011 m s^{-2} (~0.1% of gravity accelerations) with its minimum value of -456×10^{-5} m s^{-2} located in China and its maximum of 714×10^{-5} m s^{-2} expected for the Pico Cristóbal Colón summit in Colombia. The higher variability of gravity accelerations over free-air gravity reflects the well-known fact that gravity accelerations include the gravitational attraction and centrifugal effect due to Earth rotation.

The horizontal components of the gravitational field describe in approximation the North-South and East-West inclination of the quasi/geoid with respect to the reference ellipsoid. The variation range of the horizontal field components (also known as deflections of the vertical) is about ~200 arc-seconds in North South, and ~160 arc-seconds in East-West, respectively (Table 1). GGMplus reveals a candidate location for Earth's largest deflection of the vertical: about 10 km South of Annapurna II, Nepal, the plumb line is expected to deviate from the ellipsoid normal by an angle as large as ~109 arc-seconds (Fig. 3C and 3D). This translates into a most extreme quasi/geoid slope of about 0.5 m over 1 km.

4 Model evaluation

We have comprehensively compared GGMplus gravity field maps with in-situ (direct) observations of Earth's gravity field from gravimetry, astronomy, and surveying (see electronic supplementary materials). Over well-surveyed areas of North America, Europe and Australia, the comparisons suggest an accuracy level for free-air gravity and gravity accelerations of $\sim 5 \times 10^{-5}$ m s^{-2}, for horizontal field components of about 1 arc-second, and for quasigeoid heights of 0.1 m or better.

Despite the improvements conferred by recent satellite gravity to our model, the GGMplus accuracy deteriorates by a factor of ~3 to ~5 over Asia, Africa and South America which are regions with limited or very limited ground gravity data availability. Comparisons suggest a decrease in accuracy down to $\sim 20 \times 10^{-5}$ m s^{-2} for gravity, ~5 arc-seconds for horizontal field components, and ~0.3 m for quasigeoid heights. The reduced accuracy estimates mainly reflect the limited availability of gravity observations at spatial scales of ~100 to ~10 km. The accuracy of GGMplus gravity accelerations will always be lower than that of free-air gravity. This is because accelerations are directly affected by errors in the elevation data, with an elevation error of 10 m equivalent to about 3×10^{-5} m s^{-2}.

Given that any gravity field signals originating from local mass-density variations are not represented by the topographic gravity, our gravity maps cannot provide information on geological units at scales less than 10 km. This is akin to EGM2008 at spatial scales of ~30 to ~10 km over many land areas where gravity measurements are unavailable or of proprietary nature [*Pavlis et al.*, 2012]. Any global, regional or local gravity map or quasi/geoid model can only be geologically interpreted down to a resolution commensurate with the gravity observations used to construct the model. Nevertheless, incorporation of topographic gravity to approximate gravity field features at spatial scales of ~10 km to ~250 m significantly improves GGMplus gravity and horizontal components when compared to 10 km-resolution maps. Depending on the terrain ruggedness, the observed improvement rates mostly range between 40 to 90% for radial and horizontal field components (Supplementary Tables 6 and 8), while the quasigeoid improvement is best observable over rugged areas (up to 40 % improvement, Supplementary Table 9).

5 Applications

Apart from enhancing our knowledge of Earth's gravity and its variations, there are several scientific and engineering applications that require high-resolution and largely complete gravity knowledge, which is now available through GGMplus gravity maps.

The quasi/geoid plays a crucial role in modern determination of topographic heights with Global Navigation Satellite Systems (such as the Global Positioning System GPS), allowing the measurement of heights above mean sea level rather than heights above the ellipsoid [e.g., *Meyer et al.*, 2006; *Featherstone*, 2008; *Hirt et al.*, 2011]. While several regional-size quasi/geoid models of good quality are available at mostly ~2 km resolution over well-surveyed land areas (e.g., Europe, USA, Australia), GGMplus is capable of providing improved quasi/geoid information over those parts of Asia, Africa and South America, where no other source of high-resolution gravity (e.g., from airborne gravity) is available. The GGMplus quasigeoid can be suitable for water flow modelling (e.g., as required in hydro-engineering), and height transfer with satellite systems, and can be of utility for the determination of offsets among continental height systems (e.g., Australia and Europe) and their unification [e.g., *Flury and Rummel*, 2005; *Rummel*, 2012]. This in turn will allow for a more consistent comparison of sea level observations at tide gauges across the oceans. Because of incorporation of newer GOCE and GRACE satellite gravity, the GGMplus quasigeoid confers improvements at ~100 km spatial scales over parts of Asia, South America and Africa, while consideration of short-scale quasigeoid effects from topography data improves the resolution of quasigeoid heights over rugged terrain [*Hirt et al.*, 2010].

GGMplus gravity accelerations and free-air gravity are a promising data source for screening and outlier-detection of terrestrial gravity databases and aid in planning of local precision gravimetric surveys. Gravity accelerations as provided by our maps are required e.g., as a correction in the context of geodetic height systems [e.g., *Meyer et al.*, 2006], for accurate topographic mapping, in metrology for calibration of precision scales [*Torge*, 1989] and seismometers, and in observational astronomy for meteorological corrections [*Corbard et al.*, 2013]. For geophysics and the exploration industry, GGMplus may prove beneficial as novel data source for in-situ reduction of detailed gravimetric surveys, revealing locations of interest for mineral prospectivity without the need to calculate and apply further rather time-consuming reductions [*Jakoby and Smilde*, 2009] Finally, horizontal field components are required to correct the impact of the Earth's irregular gravity field, e.g., for inertial navigation at or near the Earth's surface [*Grejner-Brzezinska and Wang*, 1998], or in the context of civil engineering (e.g., precision surveys for tunnel alignment), *Featherstone and Rüeger* [2000]. All of these applications require spectrally most complete information on the gravity field.

6 Conclusions

GGMplus provides the most complete description of Earth's gravity at ultra-high resolution and near-global coverage to date. This confers immediate benefits to many applications in engineering, exploration, astronomy, surveying, and potential field geophysics. While GGMplus provides moderate additional information (because of the ultra-high resolution short-scale modelling) over areas with dense coverage of gravity stations (e.g., North America, Europe, Australia), significant improvements are provided over areas with sparse ground gravity coverage (e.g., Asia, Africa, South America). For the latter regions, GGMplus provides for the first time a complete coverage with gravity at ultra-high spatial resolution, thus providing scientific aid to many developing countries. In addition, GGMplus provides crucial information to revise current standards for the maximum range of free-fall gravity accelerations over the Earth's surface. The computerized GGMplus gravity field maps are freely available for science, education and industry via and http://ddfe.curtin.edu.au/gravitymodels/GGMplus.

Acknowledgements We are grateful to the Australian Research Council for funding (DP120102441). This work was made feasible through using advanced computational resources of the iVEC/Epic supercomputing facility (Perth, Western Australia). We thank all developers and providers of data used in this study. Full methods, and detailed evaluation results are available in the electronic supplementary information, and information on data access via the project's website http://geodesy.curtin.edu.au/research/models/GGMplus.

References

Balmino, G., N. Vales, S. Bonvalot and A. Briais (2012), Spherical harmonic modelling to ultra-high degree of Bouguer and isostatic anomalies, *J. Geod.*, 86(7), 499-520, doi: 10.1007/s00190-011-0533-4.

Becker, J.J., D.T. Sandwell, W.H.F. Smith, J. Braud, B. Binder, J. Depner, D. Fabre, J. Factor, S. Ingalls, S-H. Kim, R. Ladner, K. Marks, S. Nelson, A. Pharaoh, R. Trimmer, J. Von Rosenberg, G. Wallace and P. Weatherall (2009), Global Bathymetry and Elevation Data at 30 Arc Seconds Resolution: SRTM30_PLUS, *Marine Geod.*, 32(4), 355-371.

Corbard T., F. Morand, F. Laclarex, R. Ikhlef, and M. Meftah (2013), On the importance of astronomical refraction for modern Solar astrometric measurements, *Astr. Astrophy*., April 2, 2013.

Drinkwater, M.R., R. Floberghagen, R. Haagmans, D. Muzi, and A. Popescu (2003), GOCE: ESA's first Earth Explorer Core mission, In (eds. Beutler, G.B., M.R. Drinkwater, R. Rummel, and R. von Steiger), Earth Gravity Field from Space - from Sensors to Earth Sciences. In the Space Sciences Series of ISSI, Vol. 18, 419-432, *Kluwer Academic Publishers*, Dordrecht, Netherlands ISBN: 1-4020-1408-2.

Featherstone W.E. (2008), GNSS-based heighting in Australia: current, emerging and future issues, *J. Spat. Sci.* 53, 115-133.

Featherstone W.E., and J.M. Rüeger (2000), The importance of using deviations of the vertical for the reduction of survey data to a geocentric datum, *Australian Surveyor*, 45, 46-61.

Flury, J., and R. Rummel (2006), Future satellite gravimetry for geodesy, *Earth Moon Plan*. 94, 13-29. doi:10.1007/s11038-005-3756-7

Forsberg R., and C.C. Tscherning (1981), The use of height data in gravity field approximation by collocation, *J. Geophys. Res*, 86(B9), 7843-7854.

Forsberg, R. (1984), A study of terrain reductions, density anomalies and geophysical inversion methods in gravity field modelling, Report 355, *Department of Geodetic Science and Surveying*, Ohio State University, Columbus.

Grejner-Brzezinska, D.A., and J. Wang (1998), Gravity modeling for high-accuracy GPS/INS integration, *Navigation*, 45, 3, 209-220.

Hirt, C. (2010), Prediction of vertical deflections from high-degree spherical harmonic synthesis and residual terrain model data, J. *Geod.*, 84 (3), 179-190. doi:10.1007/s00190-009-0354-x

Hirt, C., W.E. Featherstone and U. Marti (2010), Combining EGM2008 and SRTM/DTM2006.0 residual terrain model data to improve quasigeoid computations in mountainous areas devoid of gravity data, *J. Geod.*, 84(9): 557-567, DOI: 10.1007/s00190-010-0395-1..

Hirt C., Schmitz M., Feldmann-Westendorff U., Wübbena G., Jahn C.-H., and Seeber G. (2011), Mutual validation of GNSS height measurements from high-precision geometric-astronomical levelling, *GPS Solutions*, 15(2), 149-159, DOI 10.1007/s10291-010-0179-3.

Hirt, C. (2012), Efficient and accurate high-degree spherical harmonic synthesis of gravity field functionals at the Earth's surface using the gradient approach, *J. Geod.*, 86(9), 729-744, doi: 10.1007/s00190-012-0550-y.

Hirt, C. (2013), RTM gravity forward-modeling using topography/bathymetry data to improve high-degree global geopotential models in the coastal zone, *Marine Geod.*, 36(2):1-20, doi:10.1080/01490419.2013.779334.

Jacoby, W., and P.L. Smilde (2009), *Gravity interpretation*, Springer, Berlin, Heidelberg.

Jarvis, A., H.I. Reuter, A. Nelson, and E. Guevara (2008), Hole-filled SRTM for the globe Version 4, *Available from the CGIAR-SXI SRTM 90m database*. Available at: http://srtm.csi.cgiar.org.

Kuhn, M., W.E. Featherstone, and J.F. Kirby (2009), Complete spherical Bouguer gravity anomalies over Australia, *Australian J. Earth Sci.*, 56, 213-223.

Mohr P. J., and B.N. Taylor (2005), CODATA recommended values of the fundamental physical constants: 2002, Rev. Mod. Phys. 77 (Jan 2005).

Moritz, H. (2000), Geodetic Reference System 1980. J. Geod., 74, 128-140.

Meyer T.H., D.R. Roman, and D.B. Zilkoski (2006), What Does Height Really Mean? Part IV: GPS Heighting. *Surveying Land Inf. Sci.* 66, 165-183.

Mayer-Gürr, T., E. Kurtenbach, and A. Eicker (2010), ITG-Grace2010 Gravity Field Model. URL: http://www.igg.uni-bonn.de/apmg/index.php?id=itg-grace2010, 2010.

Pail, R., Goiginger, H., W.-D. Schuh, E. Höck, J.M. Brockmann, T. Fecher, T. Gruber, T. Mayer-Gürr, J. Kusche, A. Jäggi, and D Rieser (2010), Combined satellite gravity field model GOCO01S derived from GOCE and GRACE, *Geophys. Res. Lett.* 37, L20314, doi: 10.1029/2010GL044906.

Pail, R., S. Bruinsma, F. Migliaccio, C. Förste, H. Goiginger, W.-D. Schuh, E. Höck, M. Reguzzoni, J.M. Brockmann, O. Abrikosov, M. Veicherts, T. Fecher, R. Mayrhofer, I. Krasbutter, F. Sansò, and C.C. Tscherning (2011), First GOCE gravity field models derived by three different approaches, *J Geod.*, 85(11), 819-843, doi: 10.1007/s00190-011-0467-x.

Pavlis N.K., S.A. Holmes, S.C. Kenyon, and J.K. Factor (2012), The development and evaluation of the Earth Gravitational Model 2008 (EGM2008), *J. Geophys. Res.*, 117, B04406, doi:10.1029/2011JB008916.

Rummel, R. (2012), Height unification using GOCE. *J. Geod. Sci.* 2, 355-362.

Sansò F., and M.G. Sideris (2013), The Local Modelling of the Gravity Field: The Terrain Effects. *Lecture Notes in Earth System Sciences* 110, 169, Springer, Berlin Heidelberg.

Tziavos, I.N., and M.G. Sideris (2013), Topographic Reductions in Gravity and Geoid Modeling. *Lecture Notes in Earth System Sciences* 110, 337-400, Springer, Berlin Heidelberg.

Torge W. (1989), *Gravimetry*, de Gruyter, Berlin, New York.

Electronic supplementary material for

New ultra-high resolution picture of Earth's gravity field

Christian Hirt[1]*, Sten Claessens[1], Thomas Fecher[2], Michael Kuhn[1], Roland Pail[2], Moritz Rexer[1,2]

[1] Western Australian Centre for Geodesy, Curtin University, Perth, Australia
[2] Institute for Astronomical and Physical Geodesy, Technical University Munich, Germany

1 General

The development of GGMplus was driven by our vision to provide for the first time widely complete gravity field knowledge on a near-global scale to users of the scientific and engineering community as well as for education purposes based on freely-available data sources.

The model development was facilitated by the availability of new satellite observations of Earth's gravity field, as well as detailed topographic elevation data (Sect. 2), availability of suitable and efficient methods for highest-resolution gravity modelling (Sect. 3) and, importantly, made possible through advanced supercomputing resources provided by the iVEC/Epic supercomputing centre of Western Australia.

Coverage

GGMplus provides computerized gravity field maps at 7.2 arc-seconds (0.002° or ~224 m in latitude direction) resolution for all land areas of Earth within ± 60° geographic latitude (as represented by SRTM, with the exception of the Southern part of Greenland), and an adjoining ~10 km marine zone along the coast lines (Fig. 1). The target resolution of GGMplus of 7.2 arc-seconds translates into a total of ~3 billion computation points within our working area. The chosen resolution allows representing the short-scale variations of the radial (gravity) and horizontal field components (deflections of the vertical).

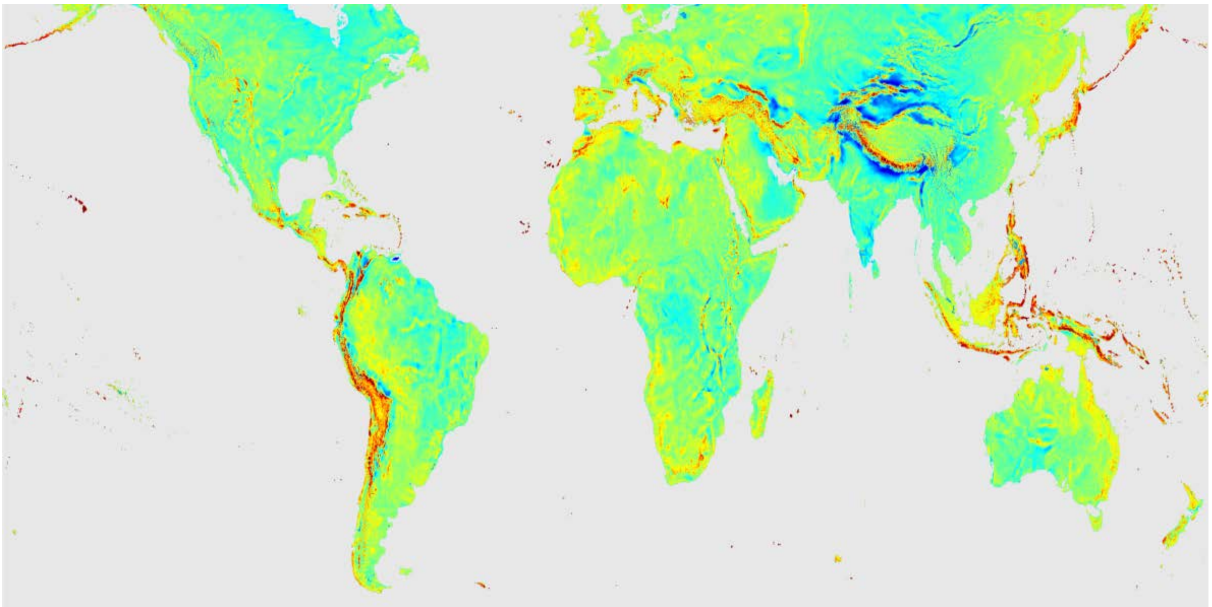

Figure 1. Coverage of GGMplus. Shown are mean values of the radial component of the gravity field over land and near-coastal areas between ± 60° geographic latitude.

Technical definitions

The five gravity field functionals provided by GGMplus are

- Free-fall gravity accelerations (i.e. gravitational plus centrifugal accelerations)
- Gravity disturbances (radial derivatives of the disturbing potential), denoted as radial component of the gravity field in the manuscript
- North-South deflection of the vertical in Helmert definition (latitudinal derivative of the disturbing potential), denoted as horizontal component of the gravity field in the manuscript
- East-West deflection of the vertical in Helmert definition (longitudinal derivative of the disturbing potential), denoted as horizontal component of the gravity field in the manuscript
- and Molodenski quasigeoid heights.

All quantities are given at the Earth's surface as defined through the SRTM (Shuttle Radar Topography Mission) topography. Users wishing to use geoid heights instead of quasigeoid heights can do so by applying standard conversion as described, e.g., *Rapp* [1997].

2 Data sets used

A complete list of data sets used for the development of GGMplus is given in Table 1. The use of these data is further detailed in Section 3.

Table 1. Data sets used for the development of GGMplus

Dataset	**Ressource**	**Citation**

GRACE satellite gravity model ITG2010s	http://icgem.gfz-potsdam.de/ICGEM	*Mayer-Gürr et al.* [2010]
GOCE-TIM4 satellite gravity model	http://icgem.gfz-potsdam.de/ICGEM/	*Pail et al.*, [2011]
EGM2008 gravity model	http://earth-info.nga.mil/ GandG/wgs84/gravitymod/egm2008/	*Pavlis et al.*, [2012]
Gridded 250 m SRTM V4.1 release over land	http://srtm.csi.cgiar.org/	*Jarvis et al.*, [2008]
Gridded SRTM30_PLUS V7 bathymetry offshore	http://topex.ucsd.edu/WWW_html/srtm30_plus.html	*Becker et al.*, [2009]
RET2012 spherical harmonic rock-equivalent topography model	http://www.geodesy.curtin.edu.au/research/models, file Earth2012.RET2012.SHCto2160.zip	*Hirt et al.*, [2012]
Earth2012 Topo/Air spherical harmonic model of Earth's physical surface	http://www.geodesy.curtin.edu.au/research/models, file Earth2012.topo_air.SHCto2160.zip	*Hirt et al.*, [2012]

3 Methods

GGMplus is constructed as a composite model of GOCE and GRACE satellite gravity, EGM2008 and topographic gravity in the space domain. The following steps were taken to develop the model:

- Combination of GOCE and GRACE satellite gravity (Sect. 3.1)
- Combination of GOCE-GRACE combined model with EGM2008 (Sect. 3.2)
- Spherical harmonic synthesis of gravity field quantities (Sect. 3.3)
- Forward-modelling of gravity field quantities (Sect. 3.4)
- Calculation of normal gravity at the Earth's surface (Sect. 3.5)
- Combination of synthesis and forward-modelling results (Sect. 3.6)

The 250 m resolution SRTM topography [*Jarvis et al.*, 2008] is consistently used to represent Earth's physical surface in the gravity field synthesis (Sect. 3.3), forward-modelling (Sect. 3.4) and calculation of normal gravity (Sect. 3.4). In approximation, SRTM elevations are physical heights above mean sea level. In processing steps 3.3 and 3.5, heights of the topography above the ellipsoid (ellipsoidal heights) are required. These were obtained in approximation as sum of SRTM and the EGM2008 quasigeoid [*Pavlis et al.*, 2012]. The geoid-quasigeoid separation was not accounted for in the construction of SRTM ellipsoidal heights, because this effect is mostly small (cm-dm-level, up to 1-2 m in the high mountains), which play a neglegible role in 3D spherical harmonic synthesis. The parameters of the GRS80 geodetic reference system [*Moritz*, 2000] were consistently used throughout the GGMplus model development.

3.1 GOCE TIM4 and GRACE combination

The satellite-only combination model has been computed by addition of full normal equations of GRACE and GOCE.

$$\left[\sum_{i=1}^{4}(A^T\Sigma(l)^{-1}A)_{GOCE,i}+A^T\Sigma(l)^{-1}A)_{GRACE}\right]x=$$
$$\left[\sum_{i=1}^{4}(A^T\Sigma(l)^{-1}l)_{GOCE,i}+A^T\Sigma(l)^{-1}l)_{GRACE}\right]\Leftrightarrow N_{sat}x=n_{sat} \quad (1)$$

The GRACE component consists of ITG-Grace2010s [*Mayer-Gürr et al.,* 2010] up to degree/order 180, which is based on GRACE K-band range rate and kinematic orbit data covering the time span from August 2002 to August 2009. The GOCE component contains reprocessed satellite gravity gradiometry data (main diagonal components V_{XX}, V_{YY} and V_{ZZ} and off-diagonal component V_{XZ} of the gravity gradient tensor; summation i = 1, …4 in Eq. (1)) from November 2009 to June 2012, as they have also been used for the 4th release of the GOCE TIM model [*Pail et al., 2011*]. In Eq. (1), l are the observations, and x the unknown spherical harmonic coefficients (SHC).

In the frame of the gravity gradient reprocessing, among others an improved algorithm for angular rate reconstruction has been applied [*Stummer et al.*, 2011], leading to a significant improvement of the gravity gradient performance mainly in the low to medium degrees [*Pail et al.*, 2013]. The resulting GOCE gradiometry normal equations are resolved up to degree/order 250.

Special emphasis has been given to realistic stochastic modeling of observation errors as part of the assembling and solution of the individual normal equation systems, yielding realistic variance-covariance information $\Sigma(l)$ for both GRACE and GOCE. In the case of GOCE, digital auto-regressive moving average (ARMA) filters have been used to set-up the variance-covariance information of the gradient observations [*Pail et al.*, 2011]. Technically, this is done by applying these filters to the full observation equation, i.e., both to the observations and the columns of the Jacobian (design matrix A). Due to the realistic stochastic modeling, the two normal equations could be combined with unit weight. Because of the further combination with EGM2008 as described in section 3.2, regularization has not been applied.

3.2 GOCE/GRACE and EGM2008 combination

The combination of the GRACE/GOCE data with EGM2008 is done on the basis of the combined GRACE/GOCE normal equations (see Sect. 3.1). Here the EGM2008 SHCs are treated as a set of *a priori* known parameters introduced into a least-squares process of the form:

$$(w_1N_{sat}+w_2\Sigma(x_{EGM})^{-1})x=w_1n_{sat}+w_2\Sigma(x_{EGM})^{-1}x_{EGM} \quad (2)$$

where x is the optimally combined set of SHCs from GRACE, GOCE and EGM2008. The terms N_{sat} and n_{sat} denote the normal equation system of GRACE/GOCE combination (cf. section 3.1), resolved up to degree/order 250.

The terms $\Sigma(x_{EGM})^{-1}$ and $\Sigma(x_{EGM})^{-1}x_{EGM}$ denote the system of normal equations, which relies exclusively on the EGM2008 coefficients x_{EGM} up to degree/order 360, which are used as pseudo-observations (the Jacobian is in this case an identity matrix). Since for EGM2008 only the variances are available, the variance-covariance matrix $\Sigma(x_{EGM})^{-1}$ has a diagonal structure. The weight for the satellite-only system is $w_1 = 1$, expressing the fact that we consider the formal errors of this combined model as correctly scaled, and the weight of EGM2008 has been assigned empirically with $w_2 = 0.16$, and the EGM2008 formal errors have been down-scaled by a factor of 1 increasing linearly to 10 in range of degrees 180 to 200. In this way, the combination is tuned giving GRACE/GOCE data dominant influence in the degrees 0 to 180 and forcing EGM2008 information to take over in the spectral range 200 to 2190, leaving the main spectral range of transition from GRACE/GOCE to EGM2008, where both components contribute significantly, between degrees 180 to 200. Figure 2 shows the relative contributions of GOCE/GRACE data (red for more than 80% GOCE/GRACE impact) and indirectly the EGM2008 model contribution (blue for more than 80% EGM2008 impact) per spherical harmonic coefficient C_{nm} / S_{nm} in the combination (for degrees 0 to 250).

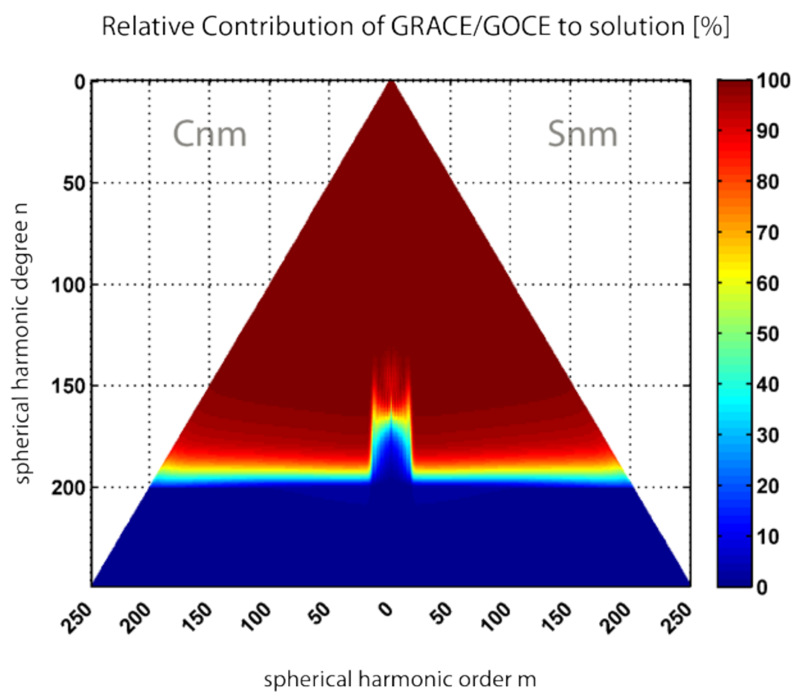

Figure 2. Relative contribution of GOCE/GRACE data per spherical harmonic coefficient C_{nm} / S_{nm} in the combination with EGM2008 data (in percent) for the degrees 0 to 250

From Fig. 2, the transition for certain harmonic orders (say -20 < m < +20) is differently than the other orders (say m<-20, m>+20). This is related to the lower accuarcy for the determination of the near-zonal spherical harmonic coefficients using GOCE gradiometry (known as the polar gap problem due to the GOCE satellite's orbit inclination of 96.6 degrees). he lack of observations in the polar regions worsens the accuracy in the determination of a certain group of spherical harmonic coefficients, which is the near-zonal group (e.g., Sneeuw and Gelderen, 1997). Consequently in the combined solution EGM2008 has a higher influence in for those coefficients where GOCE shows a lower performance (and thus a higher standard deviation).

The outcome of this processing step is a combined GRACE/GOCE/EGM2008 coefficient data set here denoted as GGE. Figure 3 shows the differences between gravity disturbances from GGE and EGM2008, revealing significant discrepancies at the 10-20 mGal-level over Africa, Asia and South America, while there is agreement in the mGal range over most parts of Europe, Australia and North-America. The larger discrepancies are interpreted as improvements over EGM2008 conferred by recent GRACE and GOCE data to GGMplus, see also *Pail et al.*, [2011] and *Hirt et al.*, [2012].

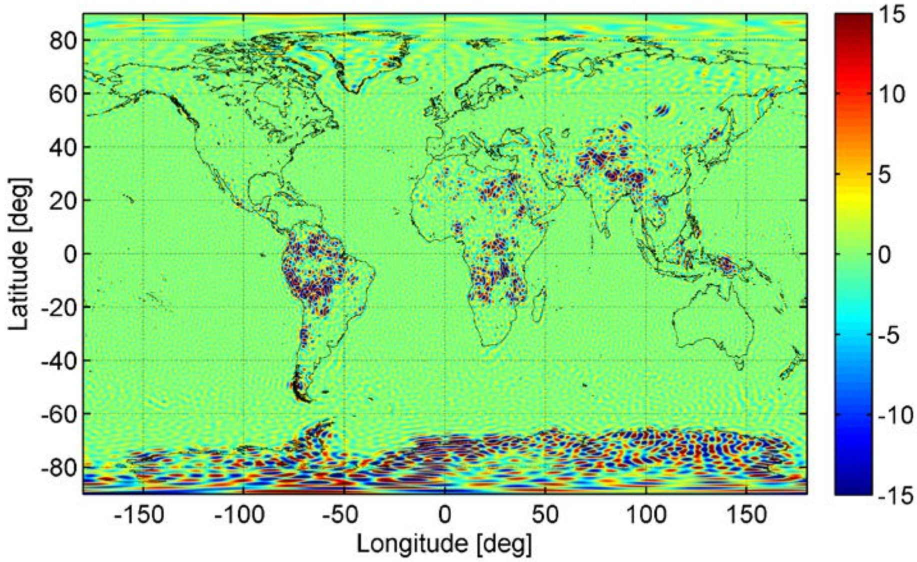

Figure 3. Gravity disturbance differences between the GRACE/GOCE/EGM2008 merger GGE and EGM2008-only in the spectral band of degrees 2 to 250, units in mGal

3.3 Synthesis

The spherical-harmonic coefficients (SHCs) of the combined GGE model were used in the spectral band of degrees 2 to 2190 to synthesize gravity field functionals at the Earth's surface, as represented through the 3D-coordinates (latitude, longitude, height). Accurate evaluation of the SHCs requires taking into account the ellipsoidal height of the evaluation points which were obtained from SRTM at 7.2 arc-second resolution. The zonal harmonics of the GRS80 normal gravity field were subtracted from the GGE-model SHCs as described in *Smith* [1998]. The tide system used in the synthesis is zero-tide, which is compatible with GRS80 [*Moritz,* 2000].

Spherical harmonic synthesis of gravity field functionals at the Earth's surface – known as 3D synthesis – is computationally extraordinarily demanding, because efficient SHS operations cannot be used [*Holmes*, 2003]. Therefore we used the gradient approach to higher order [*Hirt*, 2012] which offers an efficient yet accurate approximate solution for 3D synthesis at densely-spaced surface points, represented through the elevation model. We used a modification of the harmonic_synth software [*Holmes and Pavlis*, 2008] to synthesize quasigeoid heights, gravity disturbances, North-South and East-West deflections of the vertical at a reference height of 4 km above the GRS80 reference ellipsoid at 1 arc-min resolution. For all four functionals radial derivatives were computed up to 5th-order at the same reference height and resolution. These were bicubically interpolated to 7.2 arc-second resolution and continued from the reference height to the Earth's surface with 5th-order Taylor series expansions (cf. generic formulations provided in *Hirt* [2012]), yielding numerical estimates of gravity functionals at 3 billion surface points in the spectral band of degrees 2 to 2190.

Using the gradient approach as described, the 3D synthesis of the four gravity field functionals took about 6 weeks of computation time using an in-house Sun Ultra 45 workstation. By comparison, 3D synthesis with conventional point-by-point evaluation methods [*Holmes*, 2003] would have taken an estimated 60 years of computation time. This estimate is based on an observed performance of 100 points/ minute using the same workstation and parameters. The 3D synthesis as applied here is therefore one of the key innovations that made the construction of GGMplus feasible within acceptable computation times.

We note that the gradient approach is an approximate technique for 3D-SHS, whereby approximation errors decrease with increasing order of the Taylor series applied. From analysis of the 0th to 5th-order contributions over 3 billion points, the contribution made by subsequent orders (e.g., 0th and 1st, 1st and 2nd) differs by a factor of about 4 to 5 (see also Table 2). Given maximum contributions of 2 mm, 0.6 mGal and 0.1 arc-sec for the 5th-order, maximum approximation errors (due to truncation of the Taylor series after the 5th-order) will be generally smaller than 0.6 mm, 0.2 mGal and 0.03 arc-sec anywhere in our working area. Hence, the Taylor series as applied for GGMplus converge sufficiently, and approximation errors are negligible for practical applications.

Table 2. RMS (root-mean-square) and maximum values of the 4th-order and 5th-order terms of the Taylor expansions used for gravity field continuation to the Earth's surface. Also given are the estimated RMS and maximum approximation errors. Values reported for the functionals quasigeoid, gravity disturbances and deflections of the vertical.

Functional	Contribution of 4th –order term		Contribution of 5th –order term		Estimated approximation error	
	RMS	Max	RMS	Max	RMS	Max
Quasigeoid [mm]	0.24	9.88	0.05	2.07	0.01	0.52
Gravity [mGal]	0.06	2.54	0.01	0.59	0.00	0.15
NS deflection of the vertical [arc-sec]	0.01	0.31	0.00	0.08	0.00	0.02
EW deflection of the vertical [arc-sec]	0.01	0.34	0.00	0.08	0.00	0.02

For quasigeoid heights, the C1B correction term [*Rapp*, 1997], see also [*Hirt*, 2012], was applied to take into account the change in normal gravity with height. For gravity disturbances, the ellipsoidal correction was applied [*Claessens*, 2006]. For the North-South deflection of the vertical, corrections for the curvature of the plumbline and for the ellipsoidal effect were taken into account as described in [*Jekeli*, 1999].

3.4. Forward-modelling

Gravity forward-modelling based on high-resolution topography is a frequently-used technique to derive information on the short-scale gravity field in approximation [*Forsberg*, 1984*; Pavlis et al.*, 2007; *Hirt*, 2012]. The short-scale (i.e., 10 km to ~250 m) gravity signals of the GGMplus model are based on forward-modelling using the 7.5 arc-sec resolution (~250m) SRTM V4.1 topography [*Jarvis et al*., 2008] over land and the 30 arc-sec resolution SRTM30_PLUS V7.0 bathymetry [*Becker et al.*, 2009] over sea. A small number of bad data areas (about 0.002% of the total area covered by GGMplus as shown in Fig. 1) was identified and removed from both data sets through simple hole-filling.

The forward-modelling approach applied here follows the description given in *Hirt* [2013]. In brief, we converted the SRTM30_plus bathymetry to rock-equivalent depths before merging with the 250m SRTM V4.1 topography. The merger was high-pass filtered by subtracting heights from the RET2012 rock-equivalent topography model to degree and order 2160 (publicly available from http://geodesy.curtin.edu.au/research/models/Earth2012/, Earth2012.RET2012.SHCto2160.dat).

We applied brute-force numerical integration techniques [*Forsberg*, 1984] to convert the high-pass filtered topography (and rock-equivalent depths over sea) to topography-implied gravity, geoid and vertical deflections. The forward-modelled gravity signals possess spectral energy at spatial scales of ~10 km to ~250 m which augments GGE gravity information beyond 10 km resolution. The numerical integration was accomplished with a variant of the TC software [*Forsberg*, 1984] and an integration cap radius of 200 km around any of the ~3 billion computation points, and the correction for Earth's curvature applied, as described in *Forsberg* [1984]. Given the oscillating nature of the high-pass filtered topography, the effect of remote masses largely cancels out as pointed out by Forsberg and Tscherning [1981]. The integration radius chosen is suitable for forward-modelling of high-frequency gravity effects [*Hirt et al.*, 2010; *Hirt*, 2012].

The forward-modelling exercise was partitioned into ~19,000 computationally 'manageable' areas of 1 deg x 1 deg extension covering land areas everywhere on Earth between ± 60°-latitude with SRTM data available. Each 1 deg x 1 deg tile is composed of 625,000 computation points at 7.2 arc-seconds resolution. We utilized the iVEC/Epic supercomputing facility (http://www.ivec.org/) along with massive parallelization (simultaneous use of up to 1100 central processing units (CPUs)) to accomplish the forward-modelling for the first time near-globally. Based on non-parallelized standard computation techniques and a single CPU, the calculation of topographic gravity effects had taken an estimated 20 years, which is why all previous efforts were inevitably restricted to regional areas.

The topographic gravity effects calculations are based on the assumptions of constant mass-density (standard rock density 2670 kg/m^3) and isostatically uncompensated topography, which should well be justified given the spatial scales (less than 10 km) modelled here from topographic information (e.g., *Torge,* [2001]; *Watts,* [2001]; *Wieczorek,* [2007]). Given that any gravity field signals originating from mass-density variations [with respect to standard rock density] are not represented by the topographic gravity, our GGMplus gravity maps cannot provide geological information at scales less than 10 km. However, the same limitations apply to EGM2008 at spatial scales less than ~27 km over many developing countries [*Pavlis et al.*, 2012] and to any other gravity field model with topographic information used to increase the resolution among observed gravity.

Due to the chosen constant mass-density - often used as standard mass-density for gravity reductions in geophysics and geodesy - the chosen value should approximates well the topographically-induced gravitational attraction over granite rock (2700 kg m^{-3}), while the approximation may introduce errors up to 7% over areas of volcanic rock (2900 kg m^{-3}), and about ~26 % where sediments prevail (2000 kg m^{-3}). While inclusion of detailed mass-density maps in the forward-modelling can reduce these errors, a detailed modelling of mass-density variations was not attempted in this work because high-resolution density maps were not available everywhere in our working area.

From comparisons with ground-truth data sets, a range of studies [e.g., *Hirt et al.*, 2010; *Hirt*, 2012; *Šprlák et al.*, 2012] demonstrate that short-scale topographic gravity effects are capable of representing a significant portion (in some cases as high as 90 %) of real gravity field features over rugged terrain, see also evaluation results in Section 5.

3.5 Calculation of normal gravity at the Earth's surface

For the construction of gravity acceleration maps, normal gravity (i.e., the gravitational attraction and centrifugal acceleration generated by an oblate equipotential ellipsoid of revolution) was calculated at the Earth's surface. We used the parameters of the GRS80 reference ellipsoid [*Moritz*, 2000] along with the standard second-order Taylor expansion (*Torge* [2001], p 110, Eq. 4.63) to calculate normal gravity at the ellipsoidal heights of the Earth's surface, as represented through the SRTM topography at 7.2 arc-sec spatial resolution. Beside the gravitational attraction and centrifugal acceleration of the GRS80 mass-ellipsoid, the resulting normal gravity values also contain the effect of gravity attenuation with height (free-air effect), because we evaluated at the Earth's surface.

3.6 Combination of synthesis results, forward-modelling and normal gravity

All GGMplus gravity field functionals (quasigeoid heights, gravity disturbances, vertical deflections) are the sum of

- Synthesized functionals from the GGE SHCs (providing the spatial scales of ~10000 km down to ~10 km, Sect. 3.3) and
- Forward-modelled functionals from high-pass filtered topography/bathymetry data (providing the spatial scales from ~10 km down to ~250 m, Sect. 3.4).

GGMplus gravity accelerations were obtained as the sum of GGMplus gravity disturbances and normal gravity values (Sect 3.5).

4 Gravity estimation outside working area

Due to Earth's flattening, obvious candidate locations for Earth's maximum gravity acceleration are expected near the poles, which is outside the $\pm 60°$-SRTM latitude band. To include a likely location for Earth's maximum gravity acceleration in our work, we obtained gravity accelerations globally at 5-arc-min resolution without short-scale topographic gravity estimates, as follows:

1. We constructed a 5-arcmin grid of approximate ellipsoidal heights of the Earth's surface as the sum of elevations from the Earth2012 Topo/Air model (representing Earth's physical surface as lower interface of the atmosphere above mean sea level) and the EGM2008 quasigeoid applied as a correction.
2. We applied the gradient approach for harmonic synthesis (Sect. 3.3) to fifth-order, yielding gravity disturbances at the Earth's surface in spectral band 2 to 2190 using the GGE coefficients (Sect 3.1).
3. We calculated normal gravity at the ellipsoidal heights of the Earth's surface as described in Sect 3.5) and added the gravity disturbances, yielding gravity accelerations at 5 arc-min resolutions.

Steps 1 and 2 were applied to calculate a global 5 x 5 arc-min grid of quasigeoid heights which was then used to locate where the quasigeoid is likely to be furthest below the ellipsoid. The locations of the minimum and maximum gravity accelerations and quasigeoid heights are reported in Tables S3 and S4.

Table 3. Extreme values of gravity accelerations estimated based on 5 arc-min resolution

Extreme value	Latitude	Longitude	Value [mGal]	Comment
Minimum gravity acceleration	-9.88	-77.21	976790	GGMplus suggests a smaller value at a nearby location.
Maximum gravity acceleration	86.71	61.29	983366	Located offshore in the Arctic sea, not covered by GGMplus. Location and value reported in Table 1 in the main paper.

Table 4. Extreme values of quasigeoid heights estimated based on 5 arc-min resolution

Extreme value	Latitude	Longitude	Value [m]	Comment
Minimum quasigeoid height	4.71	78.79	-106.59	Located offshore (Laccadive Sea, South of Sri Lanka), not covered by GGMplus. Location and value reported in Table 1 in the main paper.
Maximum quasigeoid height	-4.21	138.71	86.48	GGMplus suggests a larger value at another location.

5. Model evaluation

We have evaluated GGMplus gravity field functionals using (i) gravity accelerations from terrestrial gravimetry, (ii) deflections of the vertical from geodetic-astronomical observations, and (iii) observed quasigeoid heights from GPS ellipsoidal heights and geodetic levelling (GPS/levelling). The data sets used are summarized in Table 5. Each set of observations is compared against the three modelling variants

- satellite-only gravity (GRACE combined with 4th-GOCE release) to degree and order 200 (resolution of ~100 km)
- satellite gravity combined with EGM2008 (GGE), to degree 2190 (resolution of ~10 km)
- GGMplus (resolution of ~200 m)

The descriptive statistics of the differences “observation minus model” are reported in Tables 6 and 7 for gravity disturbances, in Table 8 for deflections of the vertical and in Table 9 for quasigeoid heights. From the comparisons over North America, Europe and Australia – areas with good ground gravity coverage – the accuracy of GGMplus is at the 3-5 mGal, 1 arc-sec and 5-7 cm level or somewhat better for gravity, deflections of the vertical and quasigeoid heights, respectively. The RMS-improvements conferred by the short-scale gravity modelling (compare GGMplus with GGE) range between ~20 to ~90 % for the radial (gravity) and horizontal field components (deflections of the vertical), and is lower (non-significant to ~40% over Switzerland as an example of a mountainous region) for quasigeoid heights. Fig. 4 exemplifies the good agreement between observed gravity and GGMplus over Australia. The differences mostly reflect the effect of local mass-density variations, and can be used for geophysical interpretation. Fig. 4 also shows oscillations of 1-2 mGal amplitude and ~200 km full-wavelength which are likely to reflect the error level of GOCE satellite observations used in GGMplus.

Over less well-surveyed areas, the differences increase to ~8 to ~23 mGal, as is indicated by the few ground gravity observations available. Given that the forward-modelling of gravity effects at spatial scales of ~10 km to 200 m is based on a homogeneous procedure everywhere between ± 60° geographic latitude, there is no reason to assume a reduced performance over Asia, Africa and South America. The deterioration rather reflects the limited data availability for EGM2008 at spatial scales of ~100 to 10 km. The accuracy of GGMplus gravity field functionals is therefore largely dependent on the EGM2008 model commission errors, which can be as high as ~30-35 cm for quasigeoid heights, and ~4 arc-seconds for deflections of the vertical [*Pavlis et al.*, 2012]. We therefore expect the GGMplus accuracy to deteriorate by factor 3-5 from well-surveyed to poorly-surveyed continents.

Table 5. Gravity field observations used for evaluation of GGMplus.

Observation type	**Country/ Area**	**# Stations**	**Data source/provider**
Gravity accelerations and disturbances	United States	1,277,637	University of Texas at el Paso http://research.utep.edu/default.aspx?tabid=37229 2012 release
from terrestrial	Australia	1,625,018	Geoscience Australia

gravimetry			http://www.geoscience.gov.au 2013 release
	Switzerland	31,598	Swisstopo, Dr U Marti
	Central Africa	41,148	Bureau Gravimétrique International, Dr S Bonvalot
	India/Himalayas	7,562	Bureau Gravimétrique International, Dr S Bonvalot
	Northern South-America	12,150	Bureau Gravimétrique International, Dr S Bonvalot
Deflections of the vertical from geodetic-astronomical observations	United States	3,396	National Geodetic Survey, Drs D Smith and Y Wang
	Australia	1,063	Geoscience Australia/ Dr W Featherstone (Curtin University)
	Europe	1,056	ETZ Zurich, Dr B Bürki; Swisstopo, Dr U Marti; first author's own observations
GPS/levelling/ quasigeoid heights	United States	18972	National Geodetic Survey, http://www.ngs.noaa.gov/NGSDataExplorer/
	Germany	675	Bundesamt für Kartographie und Geodäsie, U Schirmer
	Switzerland	193	Swisstopo, Dr U Marti

Table 6. Descriptive statistics of the differences observed gravity minus models, units in mGal

Terrestrial data	Model	Min	Max	Mean	RMS
US gravity	Satellite-only	-238.85	204.19	6.83	27.41
	GGE	-271.88	110.10	-2.70	10.80
	GGMplus	-303.39	88.84	-0.68	**3.49**
Australian gravity	Satellite-only	-179.98	118.24	-1.14	14.88
	GGE	-194.33	82.65	-1.07	5.03
	GGMplus	-193.15	81.06	-0.71	**2.90**
Swiss gravity	Satellite-only	-235.04	131.13	-35.49	67.21
	GGE	-226.64	93.38	-17.59	39.72
	GGMplus	-91.23	28.71	-0.60	**4.41**

Table 7. Descriptive statistics of the differences observed gravity minus models, units in mGal

Terrestrial data	Model	Min	Max	Mean	RMS
Central Africa	Satellite-only	228.79	394.56	- 1.33	26.91
	GGE	-275.02	403.27	-0.15	9.68
	GGMplus	-284.41	399.87	0.37	**8.24**
India+ Himalayas	Satellite-only	-329.51	365.47	-5.23	43.53
	GGE	-184.46	341.92	0.04	21.84
	GGMplus	-182.44	309.74	2.45	**13.76**
Northern South-America	Satellite-only	-247.71	365.75	-11.66	66.52
	GGE	-224.32	361.48	-4.60	26.18
	GGMplus	-234.27	364.00	-0.03	**22.69**

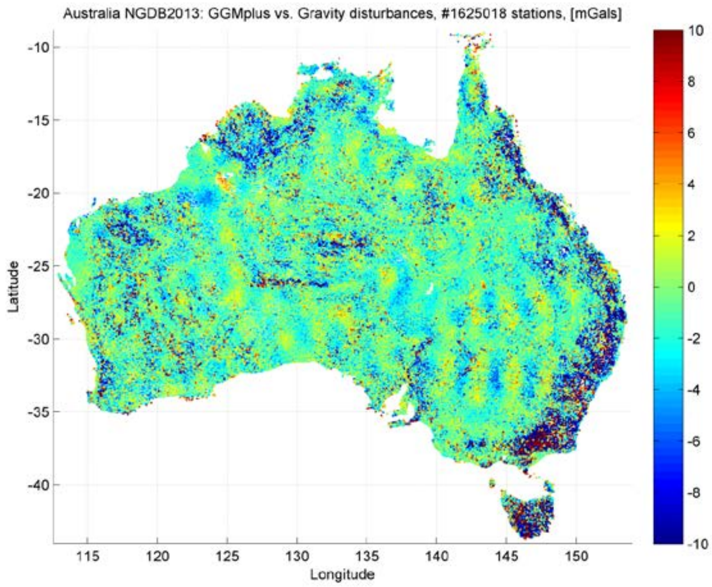

Figure 4. Differences between observed gravity accelerations and GGMplus over Australia, units in mGal.

Table 8. Descriptive statistics of the differences observed deflection of the vertical (DoV) minus models, units in arc-seconds

Terrestrial data	Model	Min	Max	Mean	RMS
US North-South DoVs	Satellite-only	-19.59	22.62	0.20	3.27
	GGE	-12.55	21.29	0.09	1.11
	GGMplus	-12.58	20.97	-0.02	**0.84**
US East-West DoVs	Satellite-only	-22.66	23.41	0.29	3.78
	GGE	-13.57	12.38	0.10	1.14
	GGMplus	-6.19	9.90	0.12	**0.78**
Australian North-South DoVs	Satellite-only	-11.58	11.76	-0.14	2.21
	GGE	-5.00	3.44	-0.23	0.81
	GGMplus	-5.13	2.61	-0.19	**0.66**
Australian East-West DoVs	Satellite-only	-18.01	11.68	-0.14	2.63
	GGE	-4.87	3.60	-0.11	1.04
	GGMplus	-5.05	4.05	-0.13	**0.97**
Europe North-South DoVs	Satellite-only	-19.49	26.96	0.88	6.41
	GGE	-15.06	15.62	0.05	3.02
	GGMplus	-4.86	5.51	-0.05	**1.06**
Europe East-West DoVs	Satellite-only	-24.05	24.97	0.90	5.87
	GGE	-11.58	15.65	0.38	2.98
	GGMplus	-4.29	4.99	0.23	**1.09**

Table 9. Descriptive statistics of the differences observed quasigeoid height minus models, units in m. In case of US GPS/levelling data, observed geoid heights were converted to quasigeoid heights applying Rapp's (1997) formalism [1] prior to comparison with the three modelling variants. A bias (Germany, Switzerland), and tilted plane (US) were subtracted.

Terrestrial data	Model	Min	Max	RMS
US GPS/lev	Satellite-only	1.80	2.72	0.367
	GGE	-0.34	0.42	**0.070**
	GGMplus	-0.36	0.43	**0.070**
German GPS/lev	Satellite-only	-1.07	1.42	0.315
	GGE	-0.11	0.17	0.042
	GGMplus	-0.10	0.14	**0.041**
Swiss GPS/lev	Satellite-only	-1.27	1.86	0.605
	GGE	-0.24	0.18	0.076
	GGMplus	-0.17	0.13	**0.046**

Additional References

Becker, J.J., D.T. Sandwell, W.H.F. Smith, J. Braud, B. Binder, J. Depner, D. Fabre, J. Factor, S. Ingalls, S-H. Kim, R. Ladner, K. Marks, S. Nelson, A. Pharaoh, R. Trimmer, J. Von Rosenberg, G. Wallace and P. Weatherall (2009), Global Bathymetry and Elevation Data at 30 Arc Seconds Resolution: SRTM30_PLUS, *Marine Geod.*, 32(4), 355-371.

Claessens, S.J., (2006), Solutions to Ellipsoidal Boundary Value Problems for Gravity Field Modelling, PhD thesis, Department of Spatial Sciences, Curtin University of Technology, Perth, Australia.

Claessens, S.J., W.E. Featherstone, I.M. Anjasmara, and M.S. Filmer (2009), Is Australian data really validating EGM2008 or is EGM2008 just in/validating Australian data, in *Newton's Bulletin* 4, 207-251 , Publication of the International Association of Geodesy and International Gravity Field Service.

Forsberg, R. (1984), A study of terrain reductions, density anomalies and geophysical inversion methods in gravity field modelling, Report 355, *Department of Geodetic Science and Surveying*, Ohio State University, Columbus.

Hirt, C. (2012), Efficient and accurate high-degree spherical harmonic synthesis of gravity field functionals at the Earth's surface using the gradient approach, *J. Geod.*, 86(9), 729-744, doi: 10.1007/s00190-012-0550-y.

Hirt, C. (2013), RTM gravity forward-modeling using topography/bathymetry data to improve high-degree global geopotential models in the coastal zone, *Marine Geod.*, 36(2):1-20, doi:10.1080/01490419.2013.779334.

Hirt C., M. Kuhn, W.E. Featherstone, and F. Goettl (2012), Topographic/isostatic evaluation of new-generation GOCE gravity field models. *J. Geophys. Res.* B05407.

Holmes, S.A., (2003), High degree spherical harmonic synthesis for simulated earth gravity modelling, PhD Thesis, Department of Spatial Sciences, Curtin University of Technology, Perth, Australia.

Holmes S.A., and N.K. Pavlis (2008), Spherical harmonic synthesis software harmonic_synth. http://earth-info.nga.mil/GandG/wgs84/gravitymod/new_egm/new_egm.html.

Jarvis, A., H.I. Reuter, A. Nelson, and E. Guevara. (2008). Hole-filled SRTM for the globe Version 4, *Available from the CGIAR-SXI SRTM 90m database*. Available at: http://srtm.csi.cgiar.org.

Jekeli C (1999), An analysis of vertical deflections derived from high-degree spherical harmonic models. *J. Geod*. 73(1), 10-22.

Mayer-Gürr, T., E. Kurtenbach, and A. Eicker (2010), ITG-Grace2010 Gravity Field Model. URL: http://www.igg.uni-bonn.de/apmg/index.php?id=itg-grace2010, 2010.

Moritz, H. (2000), Geodetic Reference System 1980. J. Geod., 74, 128-140.

Pail R., T. Fecher, M. Murböck M. Rexer, M. Stetter, T. Gruber, and C. Stummer, (2013), Impact of GOCE Level 1b data reprocessing on GOCE-only and combined gravity field models. *Stud. Geophy. Geod.* 57, 155-173.

Pavlis, N.K., J.K. Factor, and S.A. Holmes (2007), Terrain-related gravimetric quantities computed for the next EGM, in *Proceedings of the 1st International Symposium of the International Gravity Field Service* 318-323, Harita Dergersi, Istanbul.

Pavlis N.K., S.A. Holmes, S.C. Kenyon, and J.K. Factor (2012), The development and evaluation of the Earth Gravitational Model 2008 (EGM2008), *J. Geophys. Res.,* 117, B04406, doi:10.1029/2011JB008916.

Rapp R.H (1997), Use of potential coefficient models for geoid undulation determinations using a spherical harmonic representation of the height anomaly/geoid undulation difference, *J. Geod*. 71(5), 282-289.

Smith, D.A. (1998), There is no such thing as "The" EGM96 geoid: Subtle points on the use of a global geopotential model, in International Geoid Service Bulletin 8, 17-28, International Geoid Service, Milan, Italy.

Sneeuw N., van Gelderen, M. (1997), The polar gap. In: Geodetic boundary value problems in view of the one centimeter geoid. *Lecture notes in Earth Sciences*, 65, 559–568, Springer, Berlin, doi:10.1007/BFb0011699

Šprlák, M., C. Gerlach, and B.R. Pettersen, (2012), Validation of GOCE global gravity field models using terrestrial gravity data in Norway. *J. Geod. Sci.* 2, 134-143.

Stummer C., T. Fecher, and R. Pail (2013), Alternative method for angular rate determination within the GOCE gradiometer processing. *J. Geod.* 85, 585-596 (2011).

Torge, W. (2001), *Geodesy, 3rd Edition*., De Gruyter, Berlin, New York.

Watts, A.B. (2001), *Isostasy and Flexure of the Lithosphere*. Cambridge University Press.

Wieczorek M.A. (2007), Gravity and topography of the terrestrial planets, in *Treatise on Geophysics* 10, 165, Elsevier-Pergamon, Oxford.